ADVANCED FUNCTIONAL MATERIALS
www.afm-journal.de

High-Performance Dynamic Photo-Responsive Polymers With Superior Closed-Loop Recyclability

Juho Lee, Dongju Lee, Cheol-Hee Ahn, and Tae Ann Kim**

Chemical recycling to monomer (CRM) provides an ideal solution for reducing plastic waste and achieving a circular polymer economy. Cyclopentene (CP) and its derivatives are representative molecules that exemplify an efficient CRM process under mild conditions. However, most CP-based polymers possess limited thermal and mechanical properties, constraining their potential applications. Herein, new CP-based polymers with superior thermo-mechanical properties and autonomous functions are proposed by integrating anthracene as a dynamic functional motif. Anthracenes not only serve as supramolecular cross-linkages through strong π–π interactions but also form stronger chemical ones under UVA light irradiation, enhancing thermo-mechanical properties. Furthermore, damage-reporting, self-healing, and local shape reprogramming capabilities are accomplished by utilizing the reversible nature of photodimerized anthracene. A mild and orthogonal depolymerization condition for the CP-based polymers facilitates efficient monomer recovery even from mixed plastic wastes. This work presents a simple yet effective strategy to expand the usability of chemically recyclable polymers and contribute to a closed-loop polymer economy.

1. Introduction

A tremendous increase in plastic waste has urged us to explore practical methods for recycling and reuse at its end-of-life stage.[1] While mechanical recycling is the widely adopted technology for large-scale treatment of plastic waste, this process gradually degrades the material's properties through repetitive recycling processes, thereby limiting its usability in original applications and longevity.[2] In contrast, closed-loop chemical recycling also referred to as chemical recycling to monomer (CRM) or oligomer, can depolymerize already polymerized materials and convert them back into the same monomers or similar oligomers.[3–5] The polymers produced from recycled raw materials exhibit no loss of properties. Furthermore, this method allows for a reduction in the energy needed for raw materials production and a decrease in the amount of plastic waste generated from end-of-life polymers.

Among various chemical recycling methods, it is an interesting approach to utilize the thermodynamic equilibrium between monomer and polymer since it does not require any small molecules to cleave polymer bonds and allows for high purity of monomers. The key concept for this type of CRM is the ceiling temperature (T_c), at which the Gibbs free energy of polymerization equals zero.[6–9] When the reaction temperature is above T_c, depolymerization is favored and the equilibrium shifts toward a monomeric state.[10,11] This approach is primarily employed for cyclic olefin monomers or heterocyclic compounds with suitable ring strain energy, enabling reversible ring-opening and closing processes.[12,13] Cyclopentene (CP) and its derivatives are known to have superior CRM efficiency under mild conditions due to their low ring strain energy and high entropy change during polymerization.[14] However, most CP-based polymers exhibit limited thermal and mechanical properties, making them less suitable for applications requiring structural integrity. For instance, alkoxycarbonyl functionalized CPs resulted in polymers with low glass transition temperature (T_g) below 0 °C, even with bulky side groups.[15] Cross-linked polymers derived from multifunctional CPs showed a maximum modulus of less than 1 MPa.[16] Polyolefin copolymers with high styrene content synthesized from 4-phenylcyclopentene had exceptional stretchability but exhibited a low elastic modulus.[17] Hydrogenation of these copolymers doubled the elastic modulus from 0.85 to 1.61 MPa, but they lost their reversible depolymerization characteristic. Therefore, new strategies are needed to enhance the

J. Lee, D. Lee, T. A. Kim
Solutions to Electromagnetic Interference in Future-mobility Research Center
Korea Institute of Science and Technology
Seoul 02792, Republic of Korea
E-mail: takim717@kist.re.kr
J. Lee, C.-H. Ahn
Research Institute of Advanced Materials
Department of Materials and Science Engineering
Seoul National University
Seoul 08826, Republic of Korea
E-mail: chahn@snu.ac.kr
T. A. Kim
Soft Hybrid Materials Research Center
Korea Institute of Science and Technology
Seoul 02792, Republic of Korea
T. A. Kim
Division of Energy & Environment Technology
KIST School. Korea University of Science and Technology (UST)
Seoul 02792, Republic of Korea

The ORCID identification number(s) for the author(s) of this article can be found under https://doi.org/10.1002/adfm.202414842

DOI: 10.1002/adfm.202414842

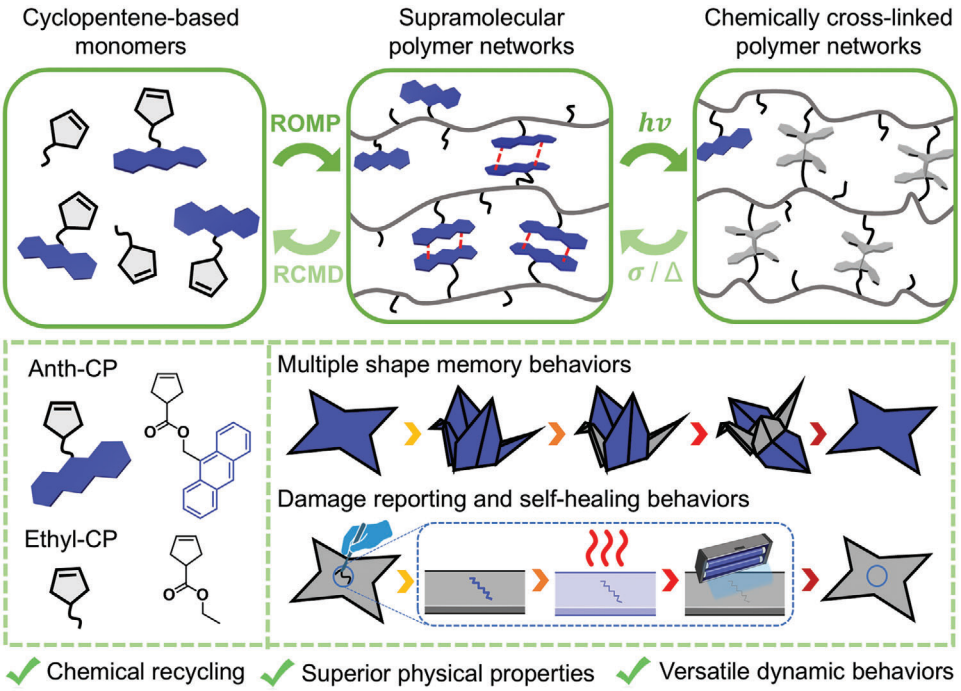

Scheme 1. Chemically recyclable and multi-functional dynamic polymers from anthracene-functionalized cyclopentene derivatives.

thermo-mechanical properties of CP-based polymers while preserving their chemical recyclability.

Dynamic bonds, which undergo reversible transformations in response to external stimuli, have been introduced into polymer materials to provide unprecedented properties that traditional polymers cannot achieve.[18–20] These dynamic motifs can be either covalent bonds that undergo reversible breaking and reformation or supramolecular interactions such as π–π stacking, hydrogen bonding, and certain metal-ligand coordination.[21] Particularly, anthracene, composed of three linearly fused aromatic rings with an extended π system of 14 delocalized electrons, is a well-known dynamic motif for designing stimuli-responsive polymers. Incorporating anthracenes into the side chains of polymers allows these molecules to form supramolecular cross-linkages through efficient π–π stacking or covalent cross-linkages through [4 + 4] cycloaddition of the middle rings between aligned anthracenes under UVA light.[22] Interestingly, this dimerization reaction is reversible; cleavage of the cycloadduct back to the parent anthracenes can be triggered by heat, mechanical force, or UVC light.[23,24] Due to their reversible nature activated by various stimuli, anthracene-containing polymers have been widely used in various applications requiring autonomous functionality, such as dynamic adhesion,[25,26] damage reporting,[27,28] self-healing,[29,30] and reversible strengthening.[31,32]

Herein, we overcome the limitations of CP-based polymers by integrating anthracene, as a dynamic side chain motif. Anthracene-functionalized CPs are synthesized and copolymerized with other CP derivatives via ring-opening metathesis polymerization (ROMP) to modulate their thermo-mechanical properties (**Scheme 1**). Unlike previously reported CP-based polymers, our synthesized copolymers exhibit significant improvements in thermo-mechanical properties due to the formation of supramolecular networks through the π–π interactions of anthracenes. Additionally, the photo-dimerization of anthracenes transforms the supramolecular cross-linkages into covalent ones, further strengthening the synthesized copolymers. The reversible nature of photodimerized anthracene enables our polymers to possess autonomous features such as damage reporting, self-healing, and multiple shape memory behaviors with local shape fixing. Finally, by demonstrating the selective retrieval of high-purity monomers through ring-closing metathesis depolymerization (RCMD) from end-of-life polymers, our study achieves its goal of maintaining the recyclability of CPs while enhancing their properties and broadening their usability.

2. Results and Discussion

The ring strain energy of CP derivatives can vary depending on the type or position of the substituent, which ultimately influences the T_c of their polymerized form.[33] Therefore, we performed density functional theory (DFT) calculations to investigate the ring strain energies (ΔE) of our designed CP derivatives, 9-anthracenylmethyl 3-cyclopentene-1-carboxylate (**Anth-CP**) and ethyl 3-cyclopentene-1-carboxylate (**Ethyl-CP**) (Figure S1 and Table S1, Supporting Information). Compared to the calculated ΔE of CP (−4.23 kcal mol^{-1}), **Anth-CP** exhibited a comparable value (−4.27 kcal mol^{-1}), while **Ethyl-CP** had a slightly higher one (−6.58 kcal mol^{-1}). Previous studies have shown that this small change in ring strain energy of CP derivatives does not affect either their reversible ring-opening/closing behavior or reactivity during copolymerization.[34,35] Encouraged by the computational calculation results, we synthesized **Anth-CP** and **Ethyl-CP** through the *Steglich* esterification reaction with a high purity,

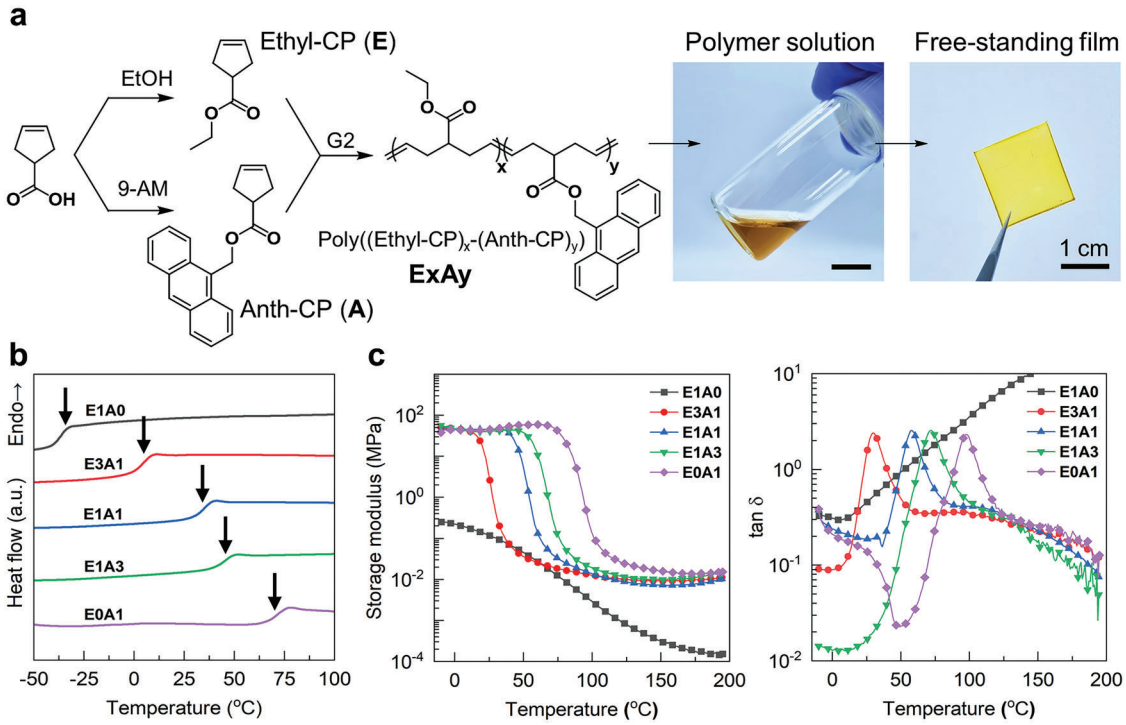

Figure 1. Anthracene-functionalized cyclopentene and its copolymers. a) Synthetic schemes for cyclopentene derivatives (**Ethyl-CP** (**E**) and **Anth-CP** (**A**)) and copolymers (**ExAy**). The resulting polymer was dissolved and then cast onto a silicone substrate, resulting in a free-standing film. b) DSC curves (T_g was indicated by a black arrow), c) Storage modulus (left), and tan δ (right) values of **ExAy**.

which was confirmed by ^{1}H and ^{13}C NMR spectroscopy (Figures S2 and S3, Supporting Information).

ROMP was conducted with our synthesized monomers using a ruthenium-based catalyst as an initiator (**Figure 1a**). The molecular weight of polymers can be controlled by adjusting the monomer to initiator ratio (Figure S4a, Supporting Information). We aimed for a molecular weight within the range of 60–70 kg mol^{-1} and synthesized five types of copolymers by varying the ratio of **Ethyl-CP** (**E**) and **Anth-CP** (**A**) (Figure S4b and Table S2, Supporting Information). The composition of copolymers exactly matched the monomer feed ratio, verified by ^{1}H NMR spectroscopy (Figure S5, Supporting Information). The sample codes (**ExAy**) were defined by the molar ratio of comonomers (**Table 1**). For instance, **E0A1** is a homopolymer consisting of **Anth-CP**, while **E1A3** is a copolymer with 25 mol% of **Ethyl-CP** and 75 mol% of **Anth-CP**. A solution drop-casting method resulted in free-standing films except for **E1A0** whose T_g was significantly lower than room temperature (−37.1 °C). Increasing the molar content of **Anth-CP** raised the T_g of the synthesized polymers up to 73.8 °C (Table 1 and Figure 1b). The thermomechanical properties of each sample were also greatly influenced by the amount of **Anth-CP** (Figure 1c). **E1A0** displayed a viscous liquid-like behavior due to a flow point below room temperature (Figure S6, Supporting Information), while other polymers containing **Anth-CP** behaved more like rubbery or glassy thermosets at room temperature with a high storage modulus (Table 1). As anticipated from the DSC results, the temperature for the glassy to rubbery transition shifted toward a higher temperature with increasing amounts of **Anth-CP**. Interestingly, polymers containing **Anth-CP** showed a stable rubbery plateau region up to 195 °C, which cannot be observed from other thermoplastic polymers. We anticipate that π–π interactions between

Table 1. Copolymers synthesized in this research.

	$M_{1,0}$ [a] [mmol]	$M_{2,0}$ [b] [mmol]	$M_{total,0}/I_0$ [c]	M_n [d] [kg mol^{-1}]	T_g [e] [°C]	T_g [f] [°C]	G′ at 25 °C [MPa]
E1A0	4.75	-	480	69.5	−37.1	−27.9	1.2×10^{-1}
E3A1	2.67	0.890	360	60.0	3.4	29.4	2.6×10^{0}
E1A1	1.48	1.48	300	69.2	33.5	57.4	4.5×10^{1}
E1A3	0.619	1.85	250	64.2	46.6	72.4	4.5×10^{1}
E0A1	-	1.98	200	69.6	73.8	97.4	4.5×10^{1}

[a] The feeding moles of **Ethyl-CP** at the initial state (t = 0); [b] The feeding moles of **Anth-CP** at the initial state (t = 0); [c] I_0 means the feeding moles of Grubbs 2nd generation catalyst at the initial state (t = 0); [d] The number-average molecular weight was determined by GPC using the PS standard; [e] Obtained from DSC; [f] Determined by a rheological analysis.

anthracenes not only restrict the mobility of the polymers but also create supramolecular cross-linking junctions between the polymer chains.[36]

The formation of strong supramolecular networks in **ExAy** was identified using frequency-sweep rheology tests (Figures S7–S10, Supporting Information). In the terminal zone, **ExAy** exhibited much smaller slopes than those expected from a single-element Maxwell model. This suggests that the inclusion of supramolecular moieties significantly hinders the terminal relaxation of the polymer chains.[37,38] Spectroscopic analysis also confirmed the presence of robust supramolecular aggregates of anthracene units in solid states. While all **Anth-CP**-containing polymers exhibited a maximum absorption ≈372 nm (Figure S11a, Supporting Information), their fluorescence behavior was significantly influenced by the amount of **Anth-CP** (Figure S11b and Table S3, Supporting Information). As the **Anth-CP** content increased in the copolymers, there was a notable bathochromic shift in maximum emission from 445 to 470 nm, indicating a greater formation of j-type anthracene aggregates. Notably, these emission peaks became broader and overlapped with **Anth-CP** contents.

Fluorescent anthracenes assembled through π–π interactions undergo the [4 + 4] photo-dimerization reaction under UVA light, transforming into non-fluorescent cycloadducts that can serve as chemical cross-linking points. These dimerized adducts can be thermally cleaved, reverting to their original structure (**Figure 2a**).[39] Initially, we measured the change in its absorbance to monitor the kinetics of the photo-dimerization reaction by irradiating UVA light to the **E0A1** solution (Figure 2b). The absorption band at 365 nm, corresponding to the π–π^* transition of anthracene units, dramatically decreased with UV exposure time, indicating the disruption in the conjugation of anthracene units. Within 5 min, almost 97% of anthracene units were dimerized in the solution state. We also evaluated the efficiency of the photo-dimerization reaction in the solid state by observing the decrease in fluorescence intensity of polymer films after UV exposure (Figure S12, Supporting Information). Even in the solid state, more than 90% of the anthracene units were converted into a non-fluorescent dimerized form. This excellent dimerization efficiency observed both in the solution and solid state of **Anth-CP** copolymers implies that strong π–π interactions of anthracenes facilitate their alignment, which is a prerequisite for an efficient photo-dimerization reaction.[40]

The UV-triggered dimerization of anthracene units in the copolymers significantly impacts the mechanical properties of chemically cross-linked **ExAy** (***c*-ExAy**). We monitored the changes in the storage modulus of each polymer above the T_g while exposing them to UV light over time (Figure 2c). The storage modulus increased by 3.5 times (***c*-E3A1**), 11.7 times (***c*-E1A1**), 17.5 times (***c*-E1A3**), and 25.3 times (***c*-E0A1**) relative to that of the polymer before UV exposure. We also conducted a temperature sweep test using these polymers to observe the changes in their thermo-mechanical properties (Figure 2d). The UV exposure notably increased the rubbery plateau modulus, forming a secondary transition region. With higher **Anth-CP** content, the secondary transition of ***c*-ExAy** appeared at higher temperatures than the T_g of the **ExAy** (Table S4, Supporting Information). This suggests that the newly formed covalent bonds between the anthracenes produce stronger and tighter linkages than the supramolecular ones, which limits the mobility of the polymer networks. We assume that the covalently linked anthracene dimers cleaved in the secondary transition region. This leads to the conclusion that the cleavage temperature can be changed greatly depending on the polymer matrix surrounding anthracenes, similar to previous reports suggesting that the thermal cleavage temperature can vary widely depending on the substituents of anthracene at the single molecule state and the polymer with different compositions and same constituents.[41]

The reversibility of anthracene dimerization reactions in **E1A1** was evaluated using UV–vis spectroscopy (Figure 2e; Figure S13, Supporting Information). Upon UVA irradiation, the absorbance at λ_{max} (maximum absorption wavelength) decreased from 2.4 to 0.5 within 10 min, indicating [4 + 4] dimerization of the anthracene units had occurred. After 60 min of thermal treatment at 150 °C in an inert environment, the characteristic peaks of the anthracenes reappeared, suggesting the cleavage of the dimerized adducts. This photodimerization and thermal cleavage cycle was repeated two more times, with most anthracene regaining their original spectrum. Interestingly, the kinetics of each reaction slowed with each cycle. We hypothesize that repeated cycles of anthracene dimerization lead to increased aggregation of anthracene units, which significantly hinders the mobility of polymer chains.

To assess the practical applicability of our dynamic polymers, we applied them as hard coating materials, which require excellent thermal stability, hardness, and elastic modulus to serve as protective layers against unexpected physical and environmental damage.[42] At first, the thermal stabilities of **E1A0** and **E0A1** were evaluated by thermogravimetric analysis (Figure S14, Supporting Information). Both polymers exhibited robust thermal stability up to 300 °C without any weight loss. This also confirms the stability of our polymers during the thermal dissociation of photodimerized anthracene in the ***c*-ExAy**. Next, we conducted nanoindentation tests to measure the changes in the hardness and elastic modulus for **ExAy** and ***c*-ExAy** depending on **Anth-CP** content and cross-linking type. The force required to indent to the same depth was measured (Figure S15, Supporting Information), and the calculated hardness and reduced elastic modulus are presented in **Figure 3a** and Table S5 (Supporting Information). Both **ExAy** and ***c*-ExAy** exhibited enhanced hardness and elastic modulus with increasing **Anth-CP** content since the π–π interchain interactions became stronger. When the supramolecular cross-linkages among anthracene moieties were converted into covalent bonds, the hardness and elastic modulus of ***c*-ExAy** increased compared to **ExAy** with the same amount of **Anth-CP**.[43] Specifically, **E3A1** showed exceptional enhancement in the mechanical properties after UV exposure due to its low T_g relative to the measurement condition. Most of our polymers demonstrated comparable hardness and elastic modulus to conventional polymer coating materials such as PMMA, epoxy, and PC (Figure 3b). Moreover, ***c*-E1A3** and ***c*-E0A1** exhibited higher values than engineering plastics.[44] In hard coating applications, the ability to detect damage and self-heal is crucial for maximizing the service life of coatings.[45,46] The reversible dimerization reaction of anthracenes provides this autonomous nature to our polymers. When the ***c*-ExAy** is scratched, the force-induced reversion of the [4 + 4] cycloaddition reaction occurs, reverting to the original anthracene structure. This enabled fluorescence emission solely at the damaged sites under

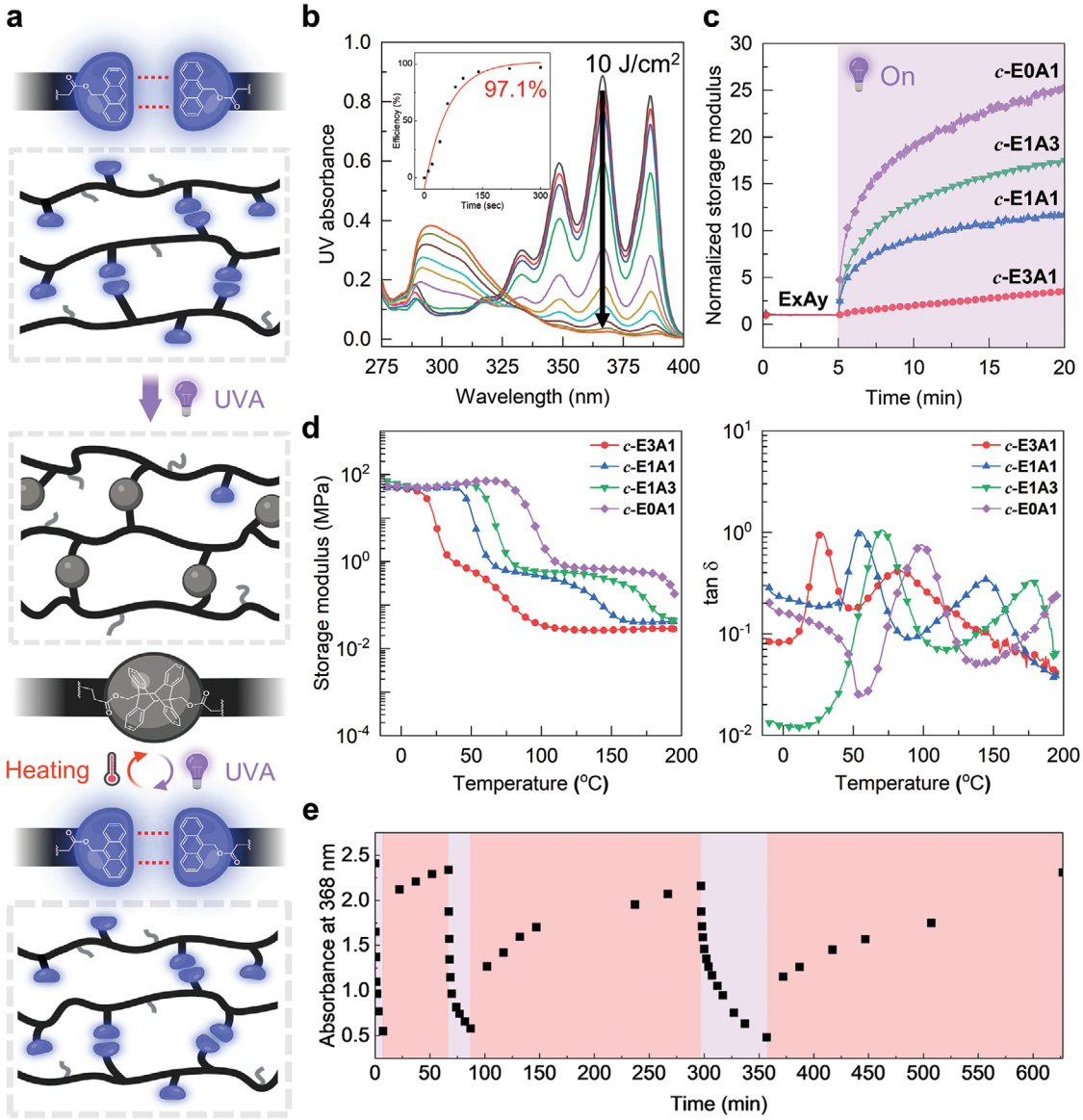

Figure 2. UV-induced chemical cross-linking and thermal cleavage of anthracenes in **ExAy**. a) Illustration of transition from supramolecular (top) to chemical cross-linking (middle) through the photo-dimerization of anthracene. The chemical cross-linked networks revert to the supramolecular networks (bottom) through the thermal dissociation process. b) Absorption spectra of **E0A1** as a function of UV irradiation time. The spectra were obtained after UV irradiation for 0, 10, 20, 40, 60, 80, 100, 140, 220, and 300 s and the photo-dimerization efficiency was calculated by the change in absorbance at 367 nm (inset). c) Increased storage moduli of chemically cross-linked **ExAy** (***c*-ExAy**) with UV irradiation time. d) Storage modulus (left) and tan δ (right) of ***c*-ExAy**. e) Changes in UV absorbance of **E1A1** upon photodimerization (purple shaded area) and thermal annealing at 150 °C (red shaded area).

UVA irradiation across all our polymers (Figure 3c). Furthermore, the damaged regions were self-healed from thermal treatment due to the reversion from chemical cross-linking to supramolecular cross-linking (Figure 3d; Figure S16, Supporting Information). To assess the self-healing behaviors of supramolecular cross-linked networks, we carried out rheological step-strain tests on **ExAy** (Figure 3e). We began with a simple strain amplitude sweep test to determine the highest and the lowest strain magnitude limits for network rupture and recovery (Figure S17, Supporting Information). Next, alternating step-strain sweeps were applied to the specimen between small (within a linear viscoelastic region) and large (above critical value) strains. While the storage modulus (G′) sharply decreased below the loss modulus (G″) at large strain, all the samples immediately restored their elasticity, regaining almost 100% of the original G′ without intervention.

To fully utilize stimuli-responsive switches in our supramolecular and chemically cross-linked polymers, we explored the shape-memory functionality of **E1A1**, which has a T_g of ≈57 °C. Once the permanent shape of **E1A1** was determined, a temporary shape was programmed by deforming the sample above its T_g and then cooling it to room temperature

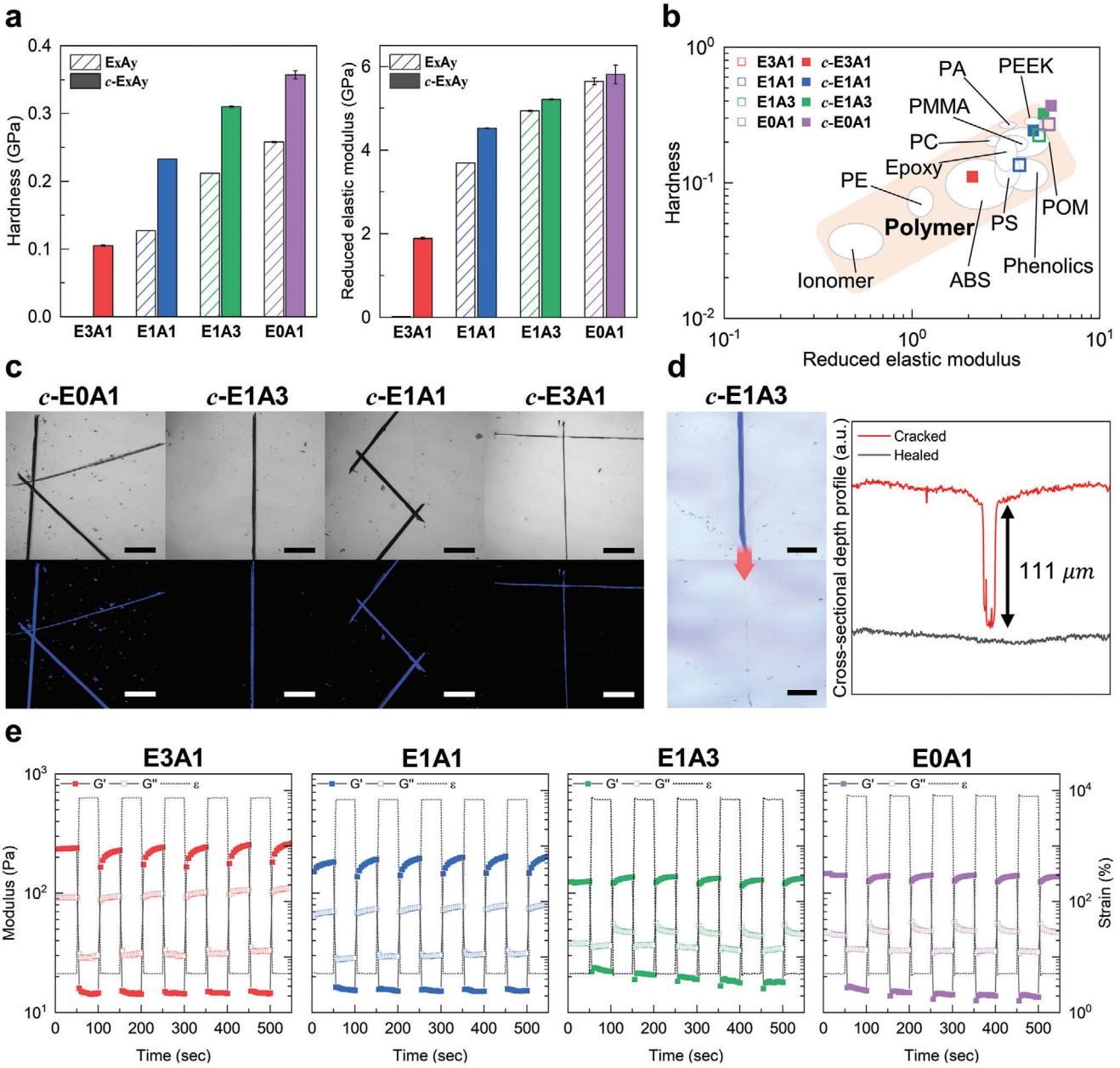

Figure 3. Applications of **ExAy** and ***c*-ExAy** to damage-reporting and self-healing coatings. a) Hardness (left) and reduced elastic modulus (right) of **ExAy** and ***c*-ExAy**. b) Ashby map of reduced elastic modulus against the hardness of **ExAy**, ***c*-ExAy**, and other representative polymers. c) Optical and fluorescence images of scratched ***c*-ExAy** samples (Scale bar = 500 μm). d) Self-healing images (left) of ***c*-E1A3** and crack depth profile (right) using a confocal laser scanning microscope (Scale bar = 500 μm). e) Cyclic step-strain tests of **ExAy** to evaluate self-healing capabilities. For all samples, alternating low (5%) and high (above flow point) strains were applied at a temperature of T_g + 60 °C.

(**Figure** 4a; Figure S18, Supporting Information). Immersing the sample in heated water (80 °C) resulted in rapid recovery of the temporary shape to its original form due to entropic elastic force (Video S1, Supporting Information). These shape memory behaviors were observed for all **Anth-CP** containing polymers and quantitatively evaluated through cyclic thermomechanical analysis (Figure 4b; Figure S19, Supporting Information). Two important parameters were obtained for describing the shape memory behaviors of the materials at a specific strain (ε_m). The shape fixity ratio (R_f) quantifies the ability to maintain a mechanical deformation of ε_m, while the shape recovery ratio (R_r) represents the ability to restore the mechanical deformation of the permanent shape (ε_p) after applying a certain deformation of ε_m. We found out that all supramolecular cross-linked polymers had an R_f value of close to 100% and an excellent shape recovery ability of ≈90% (Table S6, Supporting Information). Additionally, multi-shape programming of **E1A1** was achieved by locally converting supramolecular cross-linkages of anthracenes into

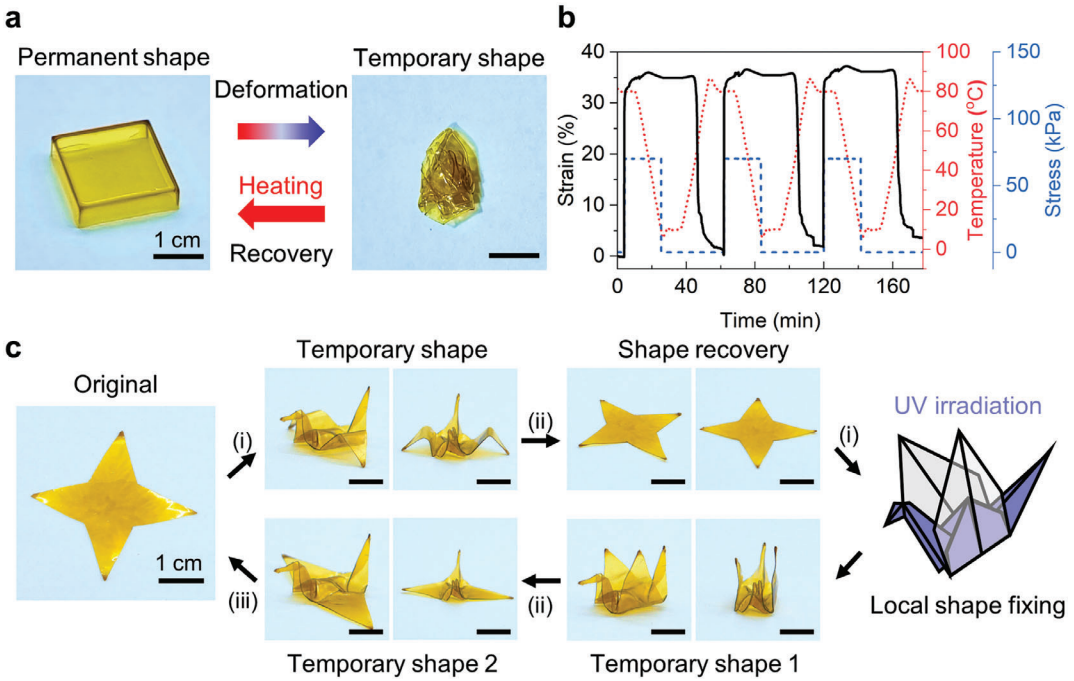

Figure 4. Evaluation of shape memory effect and local shape-programming process of **E1A1**. a) Thermal responsive dual shape memory behaviors. The temporary shape was made by deforming the sample at a temperature above its T_g and removing the applied force after cooling it to a temperature below the T_g. Then, the shape was recovered by re-heating above the T_g. b) Shape memory cyclic test under consecutive heating-cooling cycles. c) Demonstration of local shape programming and shape recovery behaviors. Step i) deformation above the T_g and cooling below the T_g. Step ii) re-heating above the T_g. Step iii) thermal cleavage of anthracene dimers above 130 °C.

covalent bonds using UVA light (Figure 4c). When a temporary shape of an origami crane was programmed with **E1A1**, reheating the sample above the T_g enabled it to recover the permanent shape. Subsequently, the origami crane was re-assembled and all parts except two wings were locally irradiated with UVA light. This prevented these parts from reverting to their permanent shape below the secondary transition temperature. The permanent shape was fully restored only when the temperature exceeded 130 °C, causing thermal cleavage of the anthracene dimers.

Our primary goal is to achieve a closed-loop chemical recycling for smart polymers with multi-functions and tunable thermomechanical properties once they reach the end of their life cycle. Depolymerization of our synthesized polymers occurs above the T_c through the ring-closing metathesis reaction catalyzed by the Grubbs 2nd-generation catalyst. The T_c can be experimentally determined by measuring the equilibrium monomer concentration ($[M]_e$) during polymerization at different temperatures, as detailed in Section S6.1 (Supporting Information). We found that **E0A1** and **E1A0** have theoretical T_c of 15.35 and −26.15 °C in solution (at $[M]_e$ = 1 M), respectively (Figure S20, Supporting Information). Based on this information, the depolymerization condition for all **ExAy** was set to 40 °C, which is significantly higher than the T_c of the two homopolymers. We first successfully demonstrated closed-loop recycling for **E0A1** (a homopolymer synthesized from **Anth-CP**), and the recovered monomers can be repolymerized without any loss of their innate properties (**Figure** 5a). Then, a representative copolymer, **E1A1**, was chemically recycled to **Anth-CP** and **Ethyl-CP** with high purity, as confirmed by the ^{1}H NMR analysis (Figure 5b; Figure S21, Supporting Information). We also evaluated the chemical recyclability of chemically cross-linked polymers. Irradiating the polymers with UVA light did not cause any unexpected side reactions, particularly to the unsaturated hydrocarbons in the backbone structures (Figure S22, Supporting Information). Both supramolecularly and chemically cross-linked polymers were successfully depolymerized with over 70% monomer conversion (Table S7, Supporting Information). Polymers containing anthracene units exhibited relatively lower conversion efficiency after UV exposure, which might be attributed to the formation of byproducts during the thermal dissociation process.[47]

Selective chemical recycling from mixed plastic wastes is important since plastic products typically consist of various polymers. Utilizing a mild and orthogonal depolymerization condition for our CP-based polymers, we conducted a model experiment to recycle **ExAy** from a mixture of common plastics such as polypropylene (PP), Nylon 6, low-density polyethylene (LDPE), polybutylene succinate (PBS), polyphenylene sulfide (PPS), and thermoplastic polyurethane (TPU). The mild recycling condition used in our research did not degrade any of the above-mentioned plastics and the monomers (**Anth-CP**, **Ethyl-CP**) were successfully recovered from plastic waste streams (Figure 5c).

3. Conclusion

In summary, we have developed photo-responsive dynamic polymers with excellent chemical recyclability by designing an anthracene-substituted cyclopentene monomer. Due to strong

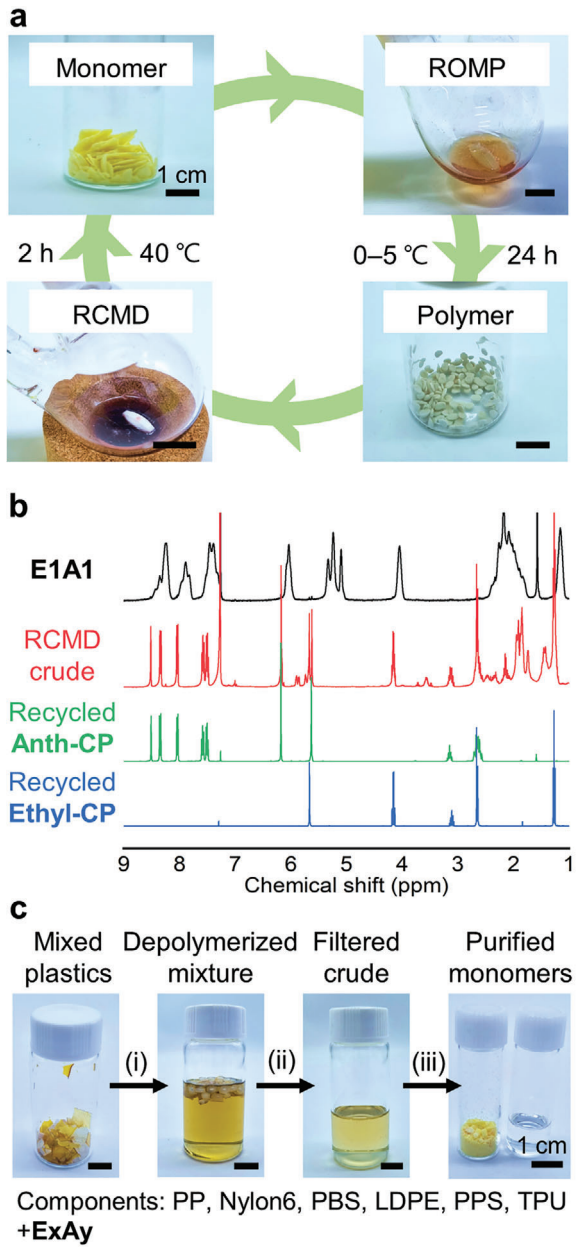

Figure 5. Closed-loop chemical recycling of **ExAy**. a) Demonstration of closed-loop chemical recycling process with **E0A1**. b) ^{1}H-NMR analysis of **E1A1**, depolymerized crude, and purified monomers after depolymerization. c) Selective chemical recycling of **ExAy**. Step i) ring-closing metathesis depolymerization (RCMD) at 40 °C for 2 h. Step ii) filtration and removal of catalysts by passing through a basic alumina column. Step iii) purification using a flash chromatography. The yellow powder (left) is **Anth-CP** and the transparent oil (right) is **Ethyl-CP**.

π–π interactions between anthracene units, our polymers exhibited superior and tunable thermo-mechanical properties depending on the amount of anthracene, surpassing conventional cyclopentene-based polymers. Upon UVA light exposure, the supramolecularly assembled anthracene units in the polymer networks transformed into non-fluorescent cycloadducts, increasing their storage modulus by up to 25.3 times compared to that of the pristine polymer. Nanoindentation tests revealed that some of our polymers had hardness and elastic modulus comparable to engineering plastics. The dimerized cycloadducts can be reversibly converted back to their fluorescent anthracene forms through mechanical force or thermal treatment, allowing these polymers to detect damage and self-heal. Furthermore, our supramolecular cross-linked polymers exhibited rapid and excellent shape memory behaviors with multi-shape programming accomplished by locally inducing photo-dimerization of anthracenes. We also demonstrated that our polymers retained the excellent chemical recyclability inherent to cyclopentene moieties and can be selectively depolymerized even from mixed plastic wastes. We envision that the novel combination of stimuli-responsive dynamic chemistry with chemically recyclable cyclic molecules could open new horizons in designing sustainable polymer materials with exceptional functionalities.

Supporting Information

Supporting Information is available from the Wiley Online Library or from the author.

Acknowledgements

The authors gratefully acknowledge the financial support provided by the National Research Council of Science & Technology (NST) grant (CRC22031-000) and the Nano & Material Technology Development Program, funded by the National Research Foundation of Korea (NRF) under the Ministry of Science and ICT (RS-2024-00448445). The authors also thank Anton Paar Korea for their assistance in obtaining in situ dynamic rheology data under UV illumination.

Conflict of Interest

The authors declare no conflict of interest.

Author Contributions

J.L. performed conceptualization, formal analysis, methodology, investigation, resources, visualization, validation, wrote the original draft. D.L. performed investigation and validation. C.-H.A. supervision, wrote, reviewed and edited the final manuscript. T.A.K. performed conceptualization, supervision, project administration, funding acquisition, wrote the original draft, reviewed and edited the final manuscript.

Data Availability Statement

The data that support the findings of this study are available from the corresponding author upon reasonable request.

Keywords

anthracene, closed-loop chemical recycling to monomer, cyclopentene, shape memory polymer, stimuli-responsive polymer

Received: August 14, 2024
Published online: September 2, 2024

[1] R. Geyer, J. R. Jambeck, K. L. Law, *Sci. Adv.* **2017**, *3*, 1700782.
[2] C. Jehanno, J. W. Alty, M. Roosen, S. De Meester, A. P. Dove, E. Y. X. Chen, F. A. Leibfarth, H. Sardon, *Nature* **2022**, *603*, 803.
[3] B. Qin, S. Liu, Z. Huang, L. Zeng, J. F. Xu, X. Zhang, *Nat. Commun.* **2022**, *13*, 7595.
[4] P. R. Christensen, A. M. Scheuermann, K. E. Loeffler, B. A. Helms, *Nat. Chem.* **2019**, *11*, 442.
[5] Q. Zhang, Y. Deng, C. Y. Shi, B. L. Feringa, H. Tian, D. H. Qu, *Matter* **2021**, *4*, 1352.
[6] J. D. Feist, Y. Xia, *J. Am. Chem. Soc.* **2020**, *142*, 1186.
[7] R. M. Cywar, N. A. Rorrer, H. B. Mayes, A. K. Maurya, C. J. Tassone, G. T. Beckham, E. Y. X. Chen, *J. Am. Chem. Soc.* **2022**, *144*, 5366.
[8] M. Hong, E. Y. X. Chen, *Nat. Chem.* **2016**, *8*, 42.
[9] C. Shi, Z. C. Li, L. Caporaso, L. Cavallo, L. Falivene, E. Y. X. Chen, *Chem* **2021**, *7*, 670.
[10] J. M. Fishman, L. L. Kiessling, *Angew. Chem. Int. Ed.* **2013**, *52*, 5061.
[11] C. M. Plummer, L. Li, Y. Chen, *Macromolecules* **2023**, *56*, 731.
[12] T. Ibrahim, A. Ritacco, D. Nalley, O. F. Emon, Y. Liang, H. Sun, *Chem. Commun.* **2024**, *60*, 1361.
[13] G. W. Coates, Y. D. Y. L. Getzler, *Nat. Rev. Mater.* **2020**, *5*, 501.
[14] W. J. Neary, J. G. Kennemur, *ACS Macro Lett.* **2019**, *8*, 46.
[15] S. Song, Z. Fu, J. Xu, Z. Fan, *Polym. Chem.* **2017**, *8*, 5924.
[16] H. Liu, A. Z. Nelson, Y. Ren, K. Yang, R. H. Ewoldt, J. S. Moore, *ACS Macro Lett.* **2018**, *7*, 933.
[17] R. J. Kieber, W. J. Neary, J. G. Kennemur, *Ind. Eng. Chem. Res.* **2018**, *57*, 4916.
[18] S. Lee, J. Song, J. Cho, J. G. Son, T. A. Kim, *ACS Appl Polym Mater* **2023**, *5*, 7433.
[19] W. Zou, J. Dong, Y. Luo, Q. Zhao, T. Xie, *Adv. Mater.* **2017**, *29*, 1606100.
[20] M. B. Gordon, J. M. French, N. J. Wagner, C. J. Kloxin, *Adv. Mater.* **2015**, *27*, 8007.
[21] M. J. Webber, M. W. Tibbitt, *Nat. Rev. Mater.* **2022**, *7*, 541.
[22] J. Van Damme, F. D.u Prez, *Prog. Polym. Sci.* **2018**, *82*, 92.
[23] H. Bouas-Laurent, A. Castellan, J. P. Desvergne, R. Lapouyade, *Chem. Soc. Rev.* **2001**, *30*, 248.
[24] B. Koo, E. Nofen, A. Chattopadhyay, L. Dai, *Comput. Mater. Sci.* **2017**, *133*, 167.
[25] Y. Zhou, C. Zhang, S. Gao, W. Li, J. J. Kai, Z. Wang, *ACS Appl. Mater. Interfaces* **2021**, *13*, 50451.
[26] Z. Wang, L. Guo, H. Xiao, H. Cong, S. Wang, *Mater. Horiz.* **2020**, *7*, 282.
[27] Y. Fang, X. Du, Z. Du, H. Wang, X. Cheng, *J Mater Chem A Mater* **2017**, *5*, 8010.
[28] C. P. Kabb, C. S. O'Bryan, C. D. Morley, T. E. Angelini, B. S. Sumerlin, *Chem. Sci.* **2019**, *10*, 7702.
[29] P. Sun, Z. Shi, W. Sima, X. Tang, T. Yuan, M. Yang, H. Xu, Z. Li, *J Mater Chem C Mater* **2023**, *11*, 14217.
[30] T. Hughes, G. P. Simon, K. Saito, *ACS Appl. Mater. Interfaces* **2019**, *11*, 19429.
[31] J. F. Xu, Y. Z. Chen, L. Z. Wu, C. H. Tung, Q. Z. Yang, *Org. Lett.* **2013**, *15*, 6148.
[32] D. Han, H. Lu, W. Li, Y. Li, S. Feng, *R. S. C. Adv.* **2017**, *7*, 56489.
[33] B. M. Coia, L. A. Hudson, A. J. Specht, J. G. Kennemur, *J. Phys. Chem. A.* **2023**, *127*, 5005.
[34] R. Tuba, M. Al-Hashimi, H. S. Bazzi, R. H. Grubbs, *Macromolecules* **2014**, *47*, 8190.
[35] R. Tuba, J. Balogh, A. Hlil, M. Barłóg, M. Al-Hashimi, H. S. Bazzi, *ACS Sustain Chem Eng.* **2016**, *4*, 6090.
[36] Z. Jiang, M. L. Tan, M. Taheri, Q. Yan, T. Tsuzuki, M. G. Gardiner, B. Diggle, L. A. Connal, *Angew. Chem.* **2020**, *132*, 7115.
[37] K. E. Feldman, M. J. Kade, E. W. Meijer, C. J. Hawker, E. J. Kramer, *Macromolecules* **2009**, *42*, 9072.
[38] C. Y. Shi, D. D. He, B. Sen Wang, Q. Zhang, H. Tian, D. H. Qu, *Angew. Chem. Int. Ed.* **2023**, *62*, 202214422.
[39] T. Salzillo, A. Brillante, *CrystEngComm* **2019**, *21*, 3127.
[40] S. V. Radl, M. Roth, M. Gassner, A. Wolfberger, A. Lang, B. Hirschmann, G. Trimmel, W. Kern, T. Griesser, *Eur. Polym. J.* **2014**, *52*, 98.
[41] J. Brancart, J. Van Damme, F. Du Prez, G. Van Assche, *Phys. Chem. Chem. Phys.* **2020**, *22*, 17306.
[42] H. Jae, J. Park, J. Byun, W. S. Chi, J. H. Kim, H. W. Jung, D. Roh, *Prog. Org. Coat.* **2024**, *191*, 108416.
[43] M. Gernhardt, E. Blasco, M. Hippler, J. Blinco, M. Bastmeyer, M. Wegener, H. Frisch, C. Barner-Kowollik, *Adv. Mater.* **2019**, *31*, 1901269.
[44] G. M. Choi, J. Jin, D. Shin, Y. H. Kim, J. H. Ko, H. G. Im, J. Jang, D. Jang, B. S. Bae, *Adv. Mater.* **2017**, *29*, 1700205.
[45] S. Yoon, J. H. Choi, B. J. Sung, J. Bang, T. A. Kim, *NPG Asia Mater* **2022**, *14*, 61.
[46] S. Bode, L. Zedler, F. H. Schacher, B. Dietzek, M. Schmitt, J. Popp, M. D. Hager, U. S. Schubert, *Adv. Mater.* **2013**, *25*, 1634.
[47] G. Collet, T. Lathion, C. Besnard, C. Piguet, S. Petoud, *J. Am. Chem. Soc.* **2018**, *140*, 10820.